Noise-Induced Dynamic Symmetry Breaking and Stochastic Transitions in ABA Molecules: I. Classification of Vibrational Modes

Maksym Kryvohuz and Jianshu Cao*

Department of Chemistry, Massachusetts Institute of Technology, Cambridge, Massachusetts 02139

Received: March 24, 2010

The dissipative vibrational dynamics of a symmetric triatomic ABA molecule is extensively studied in a series of three papers. The momentum-dependent rotor model is used to describe the dynamical behavior of an ABA molecule with a single 1:1 nonlinear resonant coupling. Four characteristic modes, including symmetric normal modes, asymmetric normal modes, local modes, and quasi-local modes, are identified at different energy regimes. Under the influence of thermal noise, an ABA molecule switches between the four distinct modes intermittently along its dynamic trajectory, resulting in blinking of vibrational bond energy. The statistics of these dynamic transitions (i.e., "vibrational blinking") is obtained from numerical integration of stochastic equations in this paper and will be analyzed within the theoretical framework of noise-induced symmetry breaking and activated barrier crossing in the next two papers. This study demonstrates the rich dynamic behavior of a highly nonlinear system in a dissipative environment and is instructive for understanding the stability and stochasticity of energy localization in complex systems ranging from polyatomic molecules to nanostructures and micromechanical oscillators.

I. Introduction

Vibrational motions of polyatomic molecules in condensed phases and solvent effects on energy redistribution within a solvated molecule are important questions in physical chemistry. Theories of vibrational dynamics of isolated molecules have been developed extensively during the last 50 years[1–6] and are now well-established; yet, little is known about vibrational motions of molecules in condensed phases. The dramatic effects of environmental fluctuations on the vibrational dynamics of solvated molecules lead to dynamic symmetry breaking,[7] normal-to-local mode transitions, and vibrational energy localization.[8] The dynamic transitions in vibrational behavior of ABA-type molecules induced by thermal noise are the subject of the present and two subsequent papers.

Vibrational dynamics of isolated polyatomic molecules can be described in terms of normal modes (collective oscillations of atoms) or local modes (independent bond oscillations). The normal-mode description is usually applicable at low vibrational energies where the small vibrations approximation is valid, while the local-mode description better describes experimental spectra at higher energies. The normal-mode dynamics is characterized by strong bond−bond coupling and results in complete energy exchange between bonds. The vibrational motion of atoms in this regime is collective and bears the symmetry of the molecule. In contrast, the local-mode regime is characterized by weak coupling between bonds and thus allows us to consider bond oscillations as being independent of each other. Because of the weak coupling, the energy flow between bonds in this regime is very slow, much slower than the normal-mode case,[9] or even absent from the classical point of view.[10] In the local-mode regime, once the bond is excited, the energy of the bond remains localized in that bond, while in the normal-mode regime, this energy will be transferred to another bond.

From the quantum mechanical point of view, no localization of vibrational excitation (or, in other words, no local-mode behavior) is possible since all eigenstates of the molecular Hamiltonian should be invariant under the symmetry transformations of the Hamiltonian,[11] and thus, in principle, all of them should be of normal-mode type. In the case of isolated molecules, the main difference between local-character and normal-character[11] quantum modes will be the time scale of energy transfer between bonds; in case of local-character modes, it is much slower than that in the case of normal character modes.[12] Yet, as shown in ref 11, local-character quantum modes are extremely susceptible to the symmetry-breaking perturbation and become localized even under small perturbation, while normal-character quantum modes remain delocalized when the same perturbation is added to the Hamiltonian. Such symmetry-breaking perturbation may arise from fluctuations of the thermal environment when the molecule is placed in a condensed phase. In the present paper, we consider an ABA molecule at thermal equilibrium with noisy environments and thus expect classical analysis of the molecule's vibrational dynamics to be generally valid.

Classical dynamics of nonlinear systems has a long history and was a subject of intense studies several decades ago, much of which has been already published in monographs.[1,13,14] The theoretical methods for the description of dynamics of coupled nonlinear oscillators were first developed and applied in the field of celestial mechanics.[15–17] They were then extensively applied to a wide range of problems,[14,18] including problems of chemical physics such as vibrational dynamics of multiatomic molecules and intramolecular vibrational energy transfer,[10,19–21] semiclassical quantization, calculation of vibrational eigenvalues,[22–25] and so forth. The most popular models for investigation of nonlinear dynamics included weakly coupled oscillators or nonlinear oscillators under resonant perturbation.[14,18] In both cases, system dynamics was shown to be governed by isolated linear or nonlinear resonances,[14,18,25] which appear between coupled nonlinear oscillations. For a system of coupled identical oscillators, dynamics is primarily guided by 1:1 resonance. Coupled identical oscillators with 1:1 resonance were investi-

* To whom correspondence should be addressed.

10.1021/jp102675y
Published on Web 04/22/2010

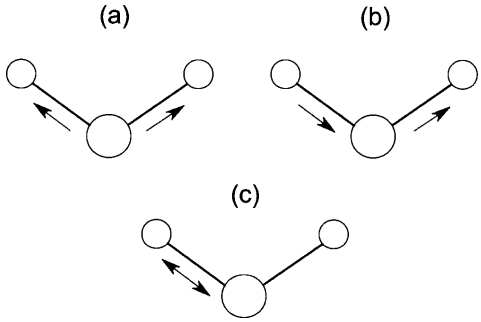

Figure 1. Stretching vibrational dynamics of ABA molecule; (a) symmetric normal mode, (b) antisymmetric normal mode, (c) local mode.

gated by many authors[10,18,23,25–30] and are also the central model of the present paper.

The vibrational dynamics of isolated ABA-type molecules has been studied extensively.[9,10,12,26–29,31–33] The simplest model of an ABA-type molecule used in the literature is two coupled Morse oscillators, which represent local AB and BA bonds with 1:1 resonance coupling between them.[9,10,18,20,29,34] From the classical point of view, local AB and BA excitations that lie within the width of the 1:1 resonance result in the normal-mode stretching vibrational motion (either symmetric or antisymmetric) and those that lie outside of the 1:1 resonance result in the local-mode picture of stretching vibrations (see Figure 1). In a particular energy range, an ABA molecule may exhibit two different types of motion, normal-mode or local-mode, depending on whether or not there is a resonance between AB and BA bonds, and may thus have a transition between these two regimes. Transitions from normal modes to local modes have been observed spectroscopically in molecules, such as in the bending mode of C_2H_2.[35] A clear local-mode behavior of the H_2S molecule at high energies was shown in experimental studies.[36] The local-mode vibrational behavior for highly excited overtones of H_2O[26] and SO_2[37] in their ground electronic states was suggested from the analysis of experimental results.

Normal-to-local mode transitions and the phase space bifurcation structure were explored by many authors.[27,28,38,39] Analysis of local-to-normal mode transitions was generally applied to isolated molecules, while the effects of the bath on small molecules were generally studied ignoring bifurcation phenomena. It is the goal of the present and subsequent papers to combine bifurcation and dissipation phenomena and to study the effect of the environment on the dynamics of a nonlinear system with bifurcations.

The effect of noise on nonlinear systems is known to result in many interesting phenomena such as activated barrier crossing,[40] stochastic resonance,[41] noise-induced transport,[42] noise-enhanced phase synchronization,[43] noise-induced transitions,[44] and so forth. In the context of physical chemistry, noise-induced dynamics was studied, for instance, in ref 45, where the relaxation of nonlinear systems coupled to a bath of environmental modes was examined, in ref 46, where chaotic dynamics of internal molecular degrees of freedom was considered as a bath to induce diffusion of the actions of the high frequency modes, and in ref 47, in which the chaotic dynamics of vibrational degrees of freedom in an ozone molecule was shown to induce diffusion of the K projection of the rotational angular momentum. The effect of chaos as a perturbing noise has been also studied in the context of Arnold diffusion,[13,18] which results in nonconservation of adiabatic invariants in weakly chaotic systems of more than two degrees of freedom. The effect of noise on coupled nonlinear oscillators was also studied for several mathematical models in numerical studies in refs 48–51. Yet, to the best of our knowledge, no theory has been proposed so far to describe noise-induced dynamical transitions in coupled nonlinear systems, such as the coupled Morse oscillator system studied here.

In a series of three papers, we discuss the effects of the thermal environment on dynamic transitions in stretching vibrational dynamics of ABA molecules. We show that under the influence of thermal noise, the stretching vibrational dynamics of an ABA-type molecule that is in thermal equilibrium with the environment continuously switches between the symmetric normal-mode (paper II,[52]), antisymmetric normal-mode, and local-mode dynamics (paper III[53]). The present paper is organized as follows; in section II, we consider the model of an isolated ABA model, which can be reduced to the model of a hindered rotor. We discuss two types of hindered rotor models, one with a momentum-independent potential, also known as a simple pendulum model, and the other with momentum-dependent potential. For the present analysis of ABA molecules in thermal equilibrium with the environment, only the momentum-dependent model is valid. Different types of vibrational modes in the ABA system, as well as their stability, are discussed in section II. The model of the dissipative ABA molecule is discussed in section III. Numerical integration of the dissipative equation of motion and the statistics of dynamical transitions are presented in section IV. We conclude with discussions in section V.

II. Isolated ABA molecule

We first review the model of nondissipative ABA molecules. The dynamics of isolated ABA molecules has been an important subject extensively investigated by many authors.[10,11,26,29] Much of our review follows their formulations and notations.

A three-atom ABA molecule is usually represented as a system of two coupled anharmonic Morse oscillators,[9,10] where each Morse oscillator represents the potential in the AB bond. The ABA Hamiltonian reads

$$H = H_1(x_1, p_1) + H_2(x_2, p_2) + G_{12}p_1p_2 \qquad \text{(II.1)}$$

where $H_i(x_i, p_i) = (1/2)G_{11}p_i^2 + U(x_i)$ is the Hamiltonian of a particle with reduced mass $1/G_{11} = 1/G_{22} = m_Am_B/(m_A + m_B)$ oscillating in the Morse potential $U(x) = D(1 - e^{-\alpha x})^2$. The coupling between the Morse potentials is of momentum−momentum type with the coupling strength $G_{12} = \cos(\theta_{ABA})/m_B$, where m_A and m_B are masses of atoms A and B, respectively, and θ_{ABA} is the angle between chemical bonds AB and BA.

The coupling term in eq II.1 can be effectively represented in action-angle variables $\{\varphi_1, J_1, \varphi_2, J_2\}$, keeping only the important 1:1 nonlinear resonance[10,29]

$$G_{12}p_1p_2 = V_0\cos(\varphi_1 - \varphi_2) \qquad \text{(II.2)}$$

where

$$V_0 = \frac{4DG_{12}}{\Omega^2 G_{11}}\omega_1\omega_2\left(\frac{1 - \frac{\omega_1}{\Omega}}{1 + \frac{\omega_1}{\Omega}}\right)^{1/2}\left(\frac{1 - \frac{\omega_2}{\Omega}}{1 + \frac{\omega_2}{\Omega}}\right)^{1/2} \qquad \text{(II.3)}$$

Thus, the Hamiltonian for ABA molecules can be rewritten in action-angle variables as

$$H = H_1(J_1) + H_2(J_2) + V_0 \cos(\varphi_1 - \varphi_2) \qquad \text{(II.4)}$$

where

$$\begin{aligned} H_i(J_i) &= D\left(1 - \left(1 - \frac{J_i}{J_b}\right)^2\right) \\ \Omega &= \sqrt{2D\alpha^2 G_{11}} \\ J_b &= \sqrt{\frac{2D}{\alpha^2 G_{11}}} \\ \omega_i &= \Omega\left(1 - \frac{J_i}{J_b}\right) \end{aligned} \qquad \text{(II.5)}$$

As shown in ref 27, the same classical expression for the Hamiltonian can be directly obtained from the quantum algebraic Hamiltonian with a Darling−Dennison coupling term.

Introducing new canonical variables[10]

$$\begin{aligned} J_+ &= J_1 + J_2 \\ J_- &= J_1 - J_2 \\ \psi_+ &= (\varphi_1 + \varphi_2)/2 \\ \psi_- &= (\varphi_1 - \varphi_2)/2 \end{aligned} \qquad \text{(II.6)}$$

we reduce Hamiltonian (eq II.4) to the form

$$H = \Omega J_+ - \frac{\Omega^2 J_+^2}{8D} - \frac{\Omega^2 J_-^2}{8D} + V_0(J_+, J_-)\cos(2\psi_-) \qquad \text{(II.7)}$$

Physically J_+ stands for the total number of vibrational quanta in ABA molecules, while J_- stands for the difference between the vibrational quanta in AB and BA bonds. For low vibrational energies, $J_i/J_b \ll 1$, we simplify V_0 to the following expression

$$\begin{aligned} V_0 &\approx 2D\frac{G_{12}}{G_{11}}\frac{1}{J_b}\sqrt{J_1 J_2} \\ &= \frac{G_{12}}{G_{11}}\frac{\Omega}{2}\sqrt{J_+^2 - J_-^2} \end{aligned} \qquad \text{(II.8)}$$

and thus obtain

$$H = \Omega J_+ - \frac{\Omega^2 J_+^2}{8D} - \frac{\Omega^2 J_-^2}{8D} + \frac{G_{12}}{G_{11}}\frac{\Omega}{2}\sqrt{J_+^2 - J_-^2}\cos(2\psi_-) \qquad \text{(II.9)}$$

J_+ is a constant of motion since the Poisson bracket is $\{H, J_+\} = 0$; thus, the effective Hamiltonian to be considered is

$$H_- \equiv \frac{\Omega^2 J_-^2}{8D} - \frac{G_{12}}{G_{11}}\frac{\Omega}{2}\sqrt{J_+^2 - J_-^2}\cos(2\psi_-) \qquad \text{(11.10)}$$

where J_+ enters as a parameter, which by definition (eq II.6) is proportional to the total energy of the ABA molecule. Introducing $W_0 = (|G_{12}|/G_{11})(\Omega/2)$ and $M = 4D/\Omega^2$, the last expression can be rewritten as

$$H_- \equiv \frac{J_-^2}{2M} + W_0\sqrt{J_+^2 - J_-^2}\cos(2\psi_-) \qquad \text{(II.11)}$$

In principle, for some molecules, the constant W_0 may also include potential coupling; yet, in the model in eq II.1, we do not consider potential coupling terms.

If $J_+ \gg J_-$, then eq II.11 can be simplified to the Hamiltonian of the hindered rotor $H_{rot} = (p^2/2M) + W_0 J_+ \cos(2\psi)$ and recovers the simple pendulum model widely discussed in refs 9, 10, and 28. Yet, this is not the case in our problem. As it will be shown below, the condition $J_+ \gg J_-$ does not apply when an ABA molecule is at thermal equilibrium with the environment (J_+ and J_- are of the same order in this case), and we need to consider momentum-dependent cosine potential $W_0(J_+^2 - p^2)^{1/2}\cos(2\psi)$ explicitly, constituting the momentum-dependent dynamic potential approach. The latter model has been previously discussed in the literature in the context of bifurcation analysis and semiclassical quantization.[24,25,27,28,30,38] In the following subsections, we will consider these two cases separately.

A. Simple Pendulum Model. We first review a simple pendulum model. The Hamiltonian of a pendulum or a hindered rotor is

$$H_{rot} = \frac{J_-^2}{2M} + U_0\cos(2\psi) \qquad \text{(II.12)}$$

where ψ is the rotation angle, $J_- = M\dot{\psi}$ stands for the rotor's angular momentum, and U_0 is a constant. Depending on the value of energy H_{rot}, there are two kinds of motion, oscillation and rotation.[10,18] For $H_{rot} < U_0$, the rotor will oscillate in the cosine potential since it does not have enough kinetic energy to overcome the potential barrier. For $H_{rot} > U_0$, the motion of the rotor is not constrained, and the type of motion is rotation. The border trajectory between oscillations and rotations, the separatrix, corresponds to $H_{rot} = U_0$ and follows the equation

$$J_-^{sx} = 2\sqrt{MU_0}\sin(\psi) \qquad \text{(II.13)}$$

The phase space representation of the hindered rotor model (eq II.12) is illustrated in Figure 2.

As discussed previously, if $J_+ \gg J_-$, the ABA Hamiltonian (eq II.11) has the form of eq II.12

$$H_{rot} = \frac{J_-^2}{2M} + W_0 J_+\cos(2\psi_-) \qquad \text{(II.14)}$$

The oscillatory motion of the rotor (eq II.14) (confined motion in the cosine potential; see Figure 2) corresponds to the normal-mode vibrational behavior of ABA molecules.[10] In this regime, J_- (rotor's momentum) periodically changes its sign, indicating continuous energy exchange between AB and BA bonds. The rotational motion of the rotor (eq II.14) corresponds to the local-mode behavior of ABA molecules. In this regime, $J_- \equiv J_1 - J_2$ always has the same sign, indicating that there is no complete energy exchange between bonds and thus each of them behaves independently.[10]

From eq II.13, we thus find the maximum value of J_- that corresponds to the normal-mode behavior of ABA molecules

$$J_-^{\max} = 2\sqrt{MW_0J_+} \tag{II.15}$$

The values of J_- higher than $J_-^{\max}$ result in unconfined rotor motion (local-mode behavior of ABA molecules). Equation II.15 stands for the width of 1:1 resonance (between AB and BA oscillators) centered at $J_1 = J_2 = J_{\text{res}} = J_+/2$.[18] In other words, for a given value of J_+ (for a given value of total energy of ABA molecule), the molecule shows normal-mode behavior if the values of J_1 and J_2 lie within the interval $(J_+/2) \pm (MW_0J_+)^{1/2}$; otherwise, the vibrational dynamics of the ABA molecule is of local-mode type. Obviously, if $(J_+/2) < (MW_0J_+)^{1/2}$, AB and BA bonds are always in resonance. Thus, we find the critical value of J_+ for the local-mode behavior[18,29]

$$\begin{aligned} J_+^{\text{c}} &= 4MW_0 \\ &= \frac{8D}{\Omega}\frac{|G_{12}|}{G_{11}} \end{aligned} \tag{II.16}$$

The lower values of J_+, $J_+ < J_+^{\text{c}}$, do not allow any local modes. In particular, the value of eq II.16 was used in ref 29 to estimate the lowest local-type excitation in the molecule of H_2O.

For actions $J_+ \gg J_+^{\text{c}}$, we have $J_+ \gg J_-^{\max}$; thus, the approximation $J_- \ll J_+$, which is necessary for the simple pendulum model, is valid only for actions J_+ sufficiently higher than the critical J_+^{c}. Yet, as we show later, this condition does not hold in the case of the dissipative ABA system at thermal equilibrium with the environment (in this case, the situation is just the opposite, $J_+ \ll J_+^{\text{c}}$), and we cannot approximate the coefficient $(J_+^2 - J_-^2)^{1/2}$ in eq II.11 with J_+; thus, the exact treatment of momentum-dependent potential is needed.

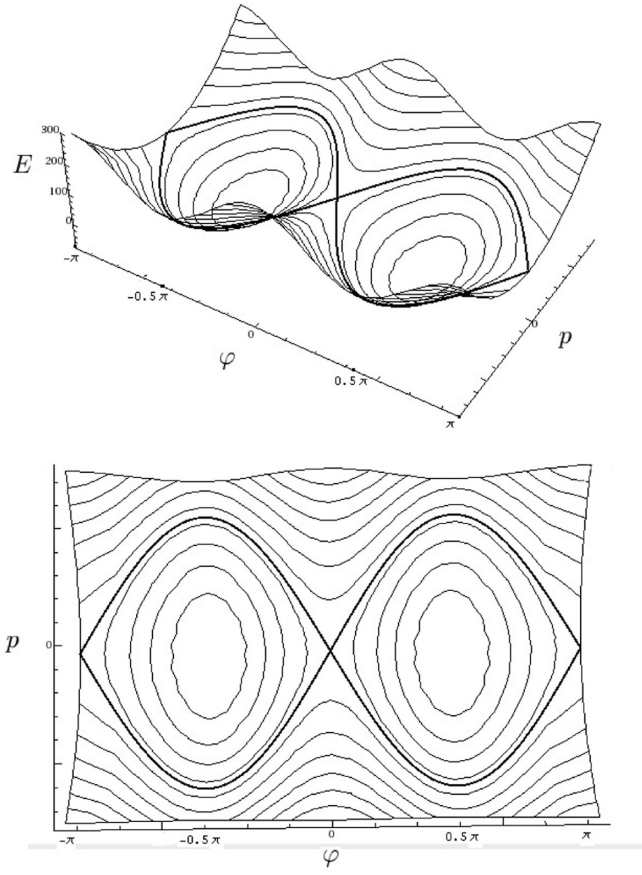

Figure 2. Phase space portrait of the hindered rotor model. As the energy E increases, trajectories become unbounded. The separatrix between oscillations (bounded motion) and rotations (unbounded motion) is shown in bold.

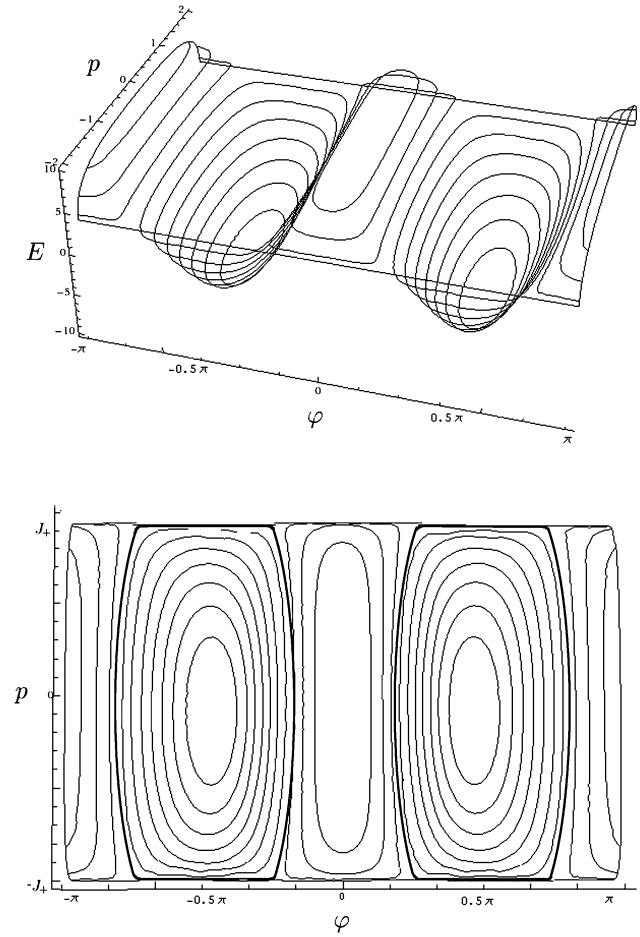

Figure 3. Phase space representation of the hindered rotor with a momentum-dependent potential, eq II.17 in the case when $J_+ < \widetilde{J_+^{\text{c}}}$. The rotor energy $E = J_+^2/2$ corresponds to the separatrix (shown in bold) between the stable oscillations around $\varphi = \pi/2 + \pi k$ (antisymmetric normal mode of ABA molecule) and the stable oscillations around $\varphi = \pi k$ (symmetric normal mode of ABA molecule). No rotational motion (unbounded trajectory) is possible for $J_+ < \widetilde{J_+^{\text{c}}}$. Thus, no local-mode behavior of ABA molecules is possible at this value of J_+; however, both symmetric and antisymmetric normal modes are stable in this case.

B. Hindered Rotor with a Momentum-Dependent Potential. The Hamiltonian (eq II.11) has the following form

$$H = \frac{J_-^2}{2M} + W_0\sqrt{J_+^2 - J_-^2}\cos(2\psi) \tag{II.17}$$

J_+ is a constant. First, we note that the maximal kinetic energy for a particle in this potential is $K_{\max} = J_+^2/2M$ because of the root in eq II.17. At energies lower than $J_+^2/2M$, the particle oscillates around the stable minimum $(\psi, J_-) = (\pi/2 + \pi k, 0)$ in the region bounded by $\psi_{\text{a}} = (1/2)\arccos(J_+/2MW_0) + \pi k$ and $\psi_{\text{b}} = \pi - (1/2)\arccos(J_+/2MW_0) + \pi k$ (see Figure 3). Since for the Hamiltonian (eq II.11) this minimum corresponds to $\psi_- = \pi/2 + \pi k$, the oscillations of ABAmolecules can be considered as antisymmetric normal-mode motion. If the energy of the rotor is higher than $J_+^2/2M$ (but lower than its maximal energy W_0J_+), the cosine potential "flips" because of the momentum dependence of its amplitude, and the oscillations

of the rotor become trapped around $\psi = \pi k$, which now corresponds to the symmetric normal-mode oscillations of ABA molecules (Figure 3). This can be seen from the linear stability analysis[38] of equations of motion

$$\frac{dJ_-}{dt} = 2W_0\sqrt{J_+^2 - J_-^2}\sin(2\psi) \qquad \text{(II.18)}$$

$$\frac{d\psi}{dt} = \frac{J_-}{M} - W_0\frac{J_-}{\sqrt{J_+^2 - J_-^2}}\cos(2\psi) \qquad \text{(II.19)}$$

The system of differential eqs II.18 and II.19 has fixed points $\dot{J}_- = 0$, $\dot{\psi} = 0$ at $(J_-, \psi) = (0, \pi n/2)$, $n = 0, \pm1, \pm2, ...$, and $(J_-, \psi) = (\pm(J_+^2 - (MW_0)^2)^{1/2}, \pi n)$. To analyze the stability of fixed points, we study the eigenvalues of stability matrix

$$M = \begin{vmatrix} -\dfrac{\partial^2 H}{\partial\psi\partial J_-} & -\dfrac{\partial^2 H}{\partial\psi^2} \\ \dfrac{\partial^2 H}{\partial J_-^2} & \dfrac{\partial^2 H}{\partial J_-\partial\psi} \end{vmatrix}$$

At points $(J_-, \psi) = (0, \pi(k + (1/2)))$, $k = \pm1, \pm2, ...$, the eigenvalues of the stability matrix are $\lambda_{1,2} = \pm(-4W_0(J_+ + MW_0)/M)^{1/2}$ and thus are purely imaginary. The point $(J_-, \psi) = (0, \pi(k + (1/2)))$ is therefore an elliptic fixed point with purely rotational phase space flow around it. For the Hamiltonian (eq II.11), this point corresponds to antisymmetric normal-mode oscillations, which are thus always stable. The fixed points $(J_-, \psi) = (0, \pi k)$, $k = 0, \pm1, \pm2, ...$, correspond to the eigenvalues $\lambda_{1,2} = \pm(4W_0(J_+ - MW_0)/M)^{1/2}$ and are purely imaginary for $J_+ < MW_0$ and real for $J_+ \geq MW_0$ and are thus either elliptic or hyperbolic (saddle) points, respectively. For the Hamiltonian in eq II.11, this point corresponds to symmetric normal-mode oscillations, which are therefore stable under certain conditions (see below). We note that for a given $J_+ < MW_0$, the Hamiltonian in eq II.17 has simultaneous stable points at $\psi = \pi k/2$ and πk. These points correspond to minima and maxima (!) of the cosine potential $\cos(2\psi)$. Since a stable motion is usually thought of as the motion around a minimum, we use the term "potential flip" when describing switching of oscillations around the points $\psi = \pi k/2$ to the oscillations around the points $\psi = \pi k$.

At the value of $J_+ = \widetilde{J_+^c} \equiv 2MW_0$, boundaries ψ_a and ψ_b (see above) coincide, and the first unbounded trajectory appears (see Figure 4). At greater values, $J_+ > \widetilde{J_+^c}$, free rotation of the rotor (unbounded trajectory) becomes possible, which suggests the appearance of local-mode behavior of ABA molecule. By comparing $\widetilde{J_+^c}$ with J_+^c from eq II.16, one can see that the model of the hindered rotor with a momentum-independent potential overestimates the critical value of J_+ 2-fold. The correct value for the critical parameter is thus

$$\widetilde{J_+^c} = 2MW_0 = \frac{4D}{\Omega}\frac{|G_{12}|}{G_{11}} \qquad \text{(II.20)}$$

and it is this parameter that determines whether the normal-to-local mode transition for ABA molecules is possible.

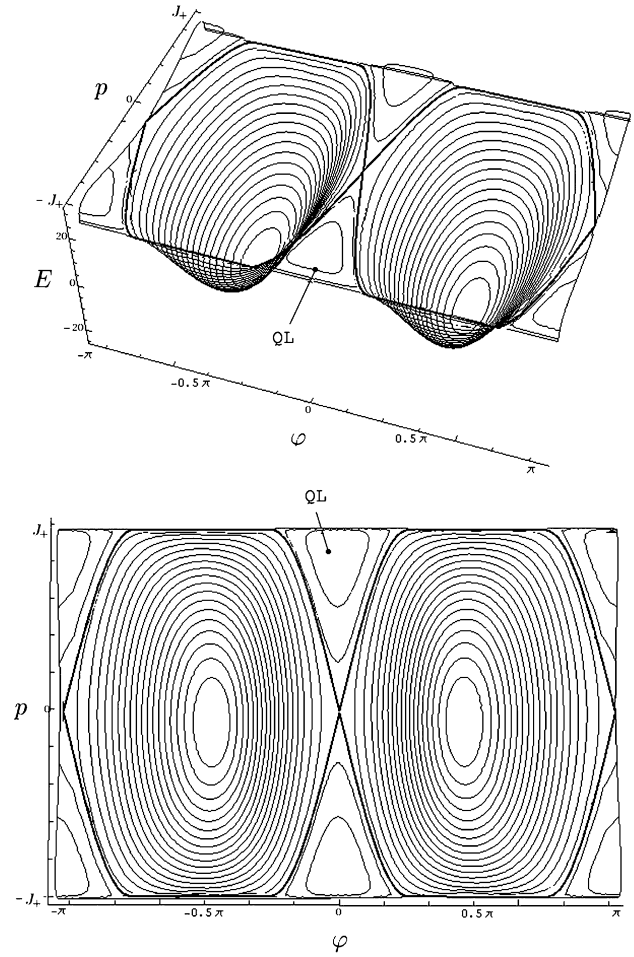

Figure 4. Phase space representation of the hindered rotor with a momentum-dependent potential, eq II.17, in the case when $J_+ = \widetilde{J_+^c}$. At this value of J_+, the first unbounded trajectory becomes possible (shown in bold), which corresponds to the appearance of local-mode behavior of the ABA molecule. The region of phase space denoted as QL corresponds to quasi-local-mode behavior of the ABA molecule (see text).

Interestingly, the remaining two fixed points at $(J_-, \psi) = (\pm(J_+^2 - (MW_0)^2)^{1/2}, \pi n)$ lead to the appearance of the islands of stability, denoted in Figure 4 as QL. They obviously are present only for the values of J_+ which are greater than or equal to

$$\widetilde{\widetilde{J_+^c}} = MW_0 = \frac{2D}{\Omega}\frac{|G_{12}|}{G_{11}} \qquad \text{(II.21)}$$

At values of J_+ higher than $\widetilde{\widetilde{J_+^c}}$, the corresponding eigenvalues of the stability matrix are $\lambda = \pm(4((MW_0)^2 - J_+^2))^{1/2}/M$, which are purely imaginary in the considered range, and therefore, the bounded motion will occur around the stable points $(J_-, \psi) = (\pm((J_+)^2 - (\widetilde{\widetilde{J_+^c}})^2)^{1/2}, \pi k)$. These oscillations correspond to the symmetric normal-mode oscillations of ABA molecule since in this case, the equilibrium value of ψ_- in the Hamiltonian in eq II.11 is πk. However, the equilibrium value of J_- in eq II.11 is now $\pm((J_+)^2 - (\widetilde{\widetilde{J_+^c}})^2)^{1/2} \neq 0$! Thus, an ABA molecule in this regime maintains energy separation between AB and BA bonds, and no energy exchange between AB and BA bonds is possible

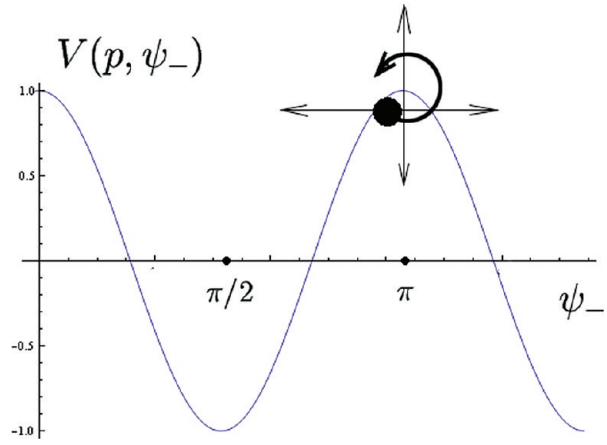

Figure 5. An illustration of the quasi-local mode. It is a motion around the closed loop, which consists of an oscillation in the potential along the horizontal axis and an oscillation of the amplitude of the cosine potential along the vertical axis. When combined together, these oscillations produce confined periodic motion with a constant-sign momentum.

(i.e., $J_- = J_1 - J_2$ never changes its sign in this regime). We thus call this regime the quasi-local-mode regime. The mechanism of confined motion with constant-sign momentum is illustrated in Figure 5 and is due to the momentum dependence of the potential surface. Both the local-mode regime and quasi-local-mode regime provide spacial localization of the vibrational energy within the bonds; see Figure 7.

The appearance of quasi-local modes and their dynamic nature have been demonstrated in the studies of isolated nonlinear systems.[28,38] Quasi-local modes were observed in ref 38 in the system of coupled Morse oscillators (see Figure 1) and correspond to the stationary phase points fp(3) and fp(4) defined there. Quasi-local modes were also observed analytically in the bifurcation analysis of the algebraic model of an ABA molecule[28] as the branches $\mu = \cos(\alpha)$ in Figure 8 of ref 28; yet, these modes were not discriminated there from the local modes. We also emphasize that the critical value $\widetilde{\widetilde{J_+^c}}$ of J_+ for the appearance of a local-mode type of dynamics in the momentum-dependent hindered rotor model (eq II.17) is 4 times less than the critical value J_+^c for the appearance of local modes in the momentum-independent hindered rotor model (eq II.12) (i.e., a simple pendulum model).

To summarize the discussion of the present section, in the following two subsections, we characterize four different types of modes that can be found in a system of two identical anharmonic oscillators coupled via 1:1 resonance term (eq II.4).

C. Antisymmetric and Symmetric Normal Modes. The system in eq II.4 oscillates in a normal-mode way if the local excitations J_1 and J_2 lie within a particular resonance zone. This resonance zone is determined by the inequality $-W_0J_+ < H_-(\psi_-, J_-, J_+) < W_0J_+$, where H_- is given by eq II.11. From the point of view of a classical dynamic potential, such energies H_- of the rotor are insufficient to overcome the dynamic potential barrier, and thus, only confined motion within the dynamic potential is possible, which constitutes the normal-mode dynamics.

If the total energy of the system is such that $(J_+^2/2M) < W_0J_+$, that is, $J_+ < J_+^c$, then the resonance zone splits into two subzones that correspond to the stable antisymmetric ($-W_0J_+ < H_-(\psi_-, J_-, J_+) < (J_+^2/2M)$) and the stable symmetric ($(J_+^2/2M) < H_-(\psi_-, J_-, J_+) < W_0J_+$) normal modes, respectively; see Figure 6. The symmetric normal mode becomes unstable for the total ABA energies when $J_+ > \widetilde{J_+^c}$.

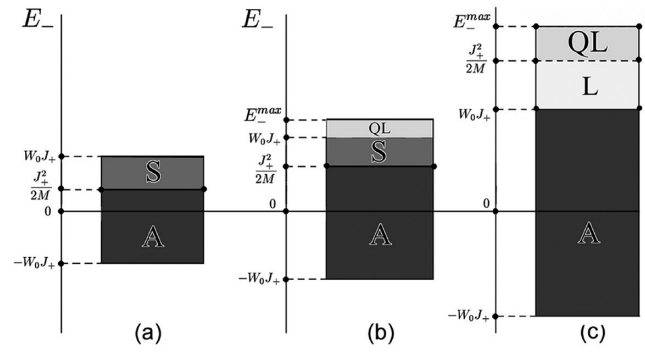

Figure 6. The allowed energies E_- of the hindered rotor system (eq II.17) and the corresponding vibrational dynamics of an ABA molecule for different values of parameter J_+; (a) $J_+ < \widetilde{\widetilde{J_+^c}}$, (b) $\widetilde{\widetilde{J_+^c}} < J_+ < \widetilde{J_+^c}$, (c) $\widetilde{J_+^c} < J_+$. The capital letters in the figure denote stable vibrational modes, antisymmetric (A), symmetric (S), quasi-local (QL), and local (L). The maximum allowed energy for the rotor is $E_-^{max} = (J_+^2 + \widetilde{\widetilde{J_+^c}}^2/2M$, $M = 4D/\Omega^2$.

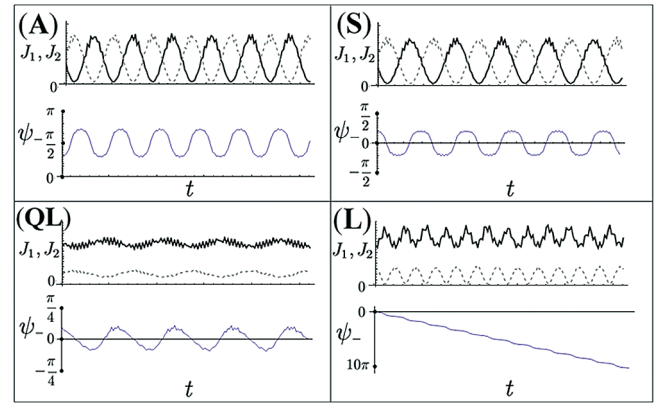

Figure 7. The typical behavior of $\psi_- \equiv (\varphi_1 - \varphi_2)/2$ and J_1 and J_2 for different types of vibrational modes, normal antisymmetric (A), normal symmetric (S), quasi-local (QL), and local (L). Here, φ_i and J_i, $i = 1$ and 2, are action-angle variables of AB and BA local bond oscillators. Solid lines in the top plots represent $J_1(t)$, and dashed lines represent $J_2(t)$. One can observe localization of J_1 and J_2 in the case of local-mode (L) and quasi-local-mode (QL) oscillations. The values of parameters were chosen from the appropriate intervals of Figure 6.

In the normal-mode regime, the phases of both Morse oscillators are constrained to oscillate either around $\psi_- = \pi/2$ in the case of the antisymmetric mode or around $\psi_- = 0$ in the case of the symmetric mode; see Figure 7. In this regime, Morse oscillators exchange their energies completely. The period of one complete exchange of Morse oscillator energies can be found as the period of oscillation in the momentum-dependent cosine potential. This period is given by[54]

$$T(E_-) = \frac{1}{2}\oint \frac{dJ_-}{\sqrt{W_0^2(J_+^2 - J_-^2) - \left(E_- - \frac{J_-^2}{2M}\right)^2}} \quad \text{(II.22)}$$

where E_- is the energy of the rotor (eq II.4).

D. Local and Quasi-Local Modes. The system in eq II.4 oscillates in the local-mode regime if the local excitations J_1 and J_2 of the Morse oscillators lie outside of the resonance zone, that is, if $W_0J_+ < H_-(\psi_-, J_-, J_+)$. The last inequality can be satisfied only for total energies such that $J_+ > \widetilde{\widetilde{J_+^c}}$; therefore, the local-mode behavior is available only for particular values

of J_+. In this way, J_+ plays a role of control parameter (see Figure 6). There are two types of local modes that we define. One is the true local mode that corresponds to the oscillations with unconstrained phases of Morse oscillators (see the bottom right plot in Figure 7), which we call the local (L) mode. The other is the type of local mode that still allows for the localization of J_1 and J_2 within the corresponding Morse oscillators (no complete exchange between J_1 and J_2) while the phases of the Morse oscillators remain constrained as in the case of the symmetric normal mode, oscillating around $\psi_- = 0$; see Figure 7. We therefore call this mode a quasi-local (QL) mode. In early ref 28, this type of mode was not distinguished from the local mode.

QL modes correspond to the islands in phase space with the energy H_- in the range of $\max\{W_0 J_+, (J_+^2/2M)\} < H_-(\psi_-, J_-, J_+) < E_-^{\max}$, where $E_-^{\max} = (1/2M)(J_+^2 + \widetilde{\widetilde{J_+^c}}^2)$ is the maximum value of $H_-(\psi_-, J_-, J_+)$ for a given $J_+ > \widetilde{\widetilde{J_+^c}}^2$. L modes correspond to the energy interval $W_0 J_+ < H_-(\psi_-, J_-, J_+) < (J_+^2/2M)$. While the phase space available for the QL modes (small islands) is much smaller than the phase space available for the L modes (unbounded trajectories), the inclusion of QL modes is important since they allow the local-mode behavior to appear at total energies of an ABA system ($J_+^{\min} = \widetilde{\widetilde{J_+^c}}$) approximately twice as low as the minimum total energy required for the L mode to appear, $J_+^{\min} = \widetilde{J_+^c} = 2\widetilde{\widetilde{J_+^c}}$.

III. ABA Molecule Coupled to the Thermal Environment

Now, we consider a dissipative ABA molecule in thermal equilibrium with the environment. One may think that at thermal equilibrium, the vibrational dynamics of ABA molecules will be of the normal-mode type since both AB and BA oscillators relax to the same thermal energy kT and thus should be always in resonance with each other. On the other hand, as we have discussed earlier, the normal-mode behavior of ABA molecules is equivalent to the confined motion in the cosine potential. It is well-known that addition of noise will lead to the escape from any potential of finite depth;[40,55] therefore, ABA molecules will switch its dynamics between normal- and local-mode behavior.

We describe the coupling to the bath in terms of a set of Harmonic oscillators[56]

$$H = H_1(x_1, p_1) + H_2(x_2, p_2) + G_{12} p_1 p_2 + \sum_j \left(\frac{P_j^2}{2} + \frac{1}{2}\omega_j^2 \left(Q_j - \frac{\gamma_j}{\omega_j^2} x_1 \right)^2 \right) + \sum_j \left(\frac{P_j'^2}{2} + \frac{1}{2}\omega_j'^2 \left(Q_j' - \frac{\gamma_j}{\omega_j'^2} x_2 \right)^2 \right) \quad \text{(III.1)}$$

We assume that AB and BA bond oscillators are subjected to independent noises from the environment. The resulting equations of motion for ABA molecules, that is, for x_1, p_1, x_2, and p_2 are

$$\begin{aligned} \frac{dx_1}{dt} &= G_{11} p_1 + G_{12} p_2 \\ \frac{dp_1}{dt} &= -\frac{dU(x_1)}{dx_1} - \int_0^t \Gamma(t-s)(G_{11} p_1(s) + G_{12} p_2)\, ds + F_1(t) \\ \frac{dx_2}{dt} &= G_{11} p_2 + G_{12} p_1 \\ \frac{dp_2}{dt} &= -\frac{dU(x_2)}{dx_2} - \int_0^t \Gamma(t-s)(G_{11} p_2(s) + G_{12} p_1)\, ds + F_2(t) \end{aligned} \quad \text{(III.2)}$$

We consider thermal noise as a white noise with friction kernel $\Gamma(t) = \gamma\delta(t)/G_{11}$ and thus having equations of motion

$$\begin{aligned} \frac{dx_1}{dt} &= G_{11} p_1 + G_{12} p_2 \\ \frac{dp_1}{dt} &= -\frac{dU(x_1)}{dx_1} - \gamma p_1 - \gamma \frac{G_{12}}{G_{11}} p_2 + F_1(t) \\ \frac{dx_2}{dt} &= G_{11} p_2 + G_{12} p_1 \\ \frac{dp_2}{dt} &= -\frac{dU(x_2)}{dx_2} - \gamma p_2 - \gamma \frac{G_{12}}{G_{11}} p_1 + F_2(t) \end{aligned} \quad \text{(III.3)}$$

where

$$\langle F(t) F(t') \rangle = \frac{2\gamma kT}{G_{11}} \delta(t - t') \quad \text{(III.4)}$$

In the present problem, we assume that the dissipative ABA molecule retains well-defined oscillating dynamics. This imposes a restriction to the allowed values of friction and temperature; both of them should be small in order to not disturb the oscillatory nature of the system, that is, $kT \ll D$ and $\gamma \ll \Omega$, or more precisely[52] $kT \ll 4D(|G_{12}|/G_{11})$ and $\gamma \ll \Omega[(|G_{12}|/G_{11})(kT/2D)]^{1/2}$. The last two inequalities result in $(J_+)/J_+^c = 2kT/\Omega J_+^c \ll 1$, indicating nonapplicability of a simple pendulum model. In the following paper,[52] we further simplify the stochastic eq III.3 and derive the effective Langevin equation in action-angle variables. In this paper, we present the numerical results obtained from the integration of eq III.3.

IV. Numerical Results

Under the influence of noise, the rotor escapes from the cosine potential, and therefore, an ABA molecule escapes from its dynamic coupling potential, breaking the symmetry of oscillations or resulting in a normal-to-local mode transition. Once in the local mode, the local excitations relax to equilibrium energies and again form a normal mode. Thus, a molecule continuously switches its type of vibrational behavior. The typical dynamic transitions can be seen in Figures 8−10, which were obtained from the integration of stochastic eq III.3 for the model of the water molecule in eq II.1. These figures represent individual types of transitions, and a single long stochastic trajectory contains all of the shown types of dynamic transitions.

The Euler integration scheme[57] was used to numerically solve the stochastic differential eq III.3. The parameters of the ABA molecule were chosen to be those of the H_2O and D_2O models given in ref 10. The parameters of the thermal environment varied from 1/75 to 1/1000 for kT/D and from 1/2000 to 1/12000 for γ/Ω, in accordance with the discussion at the end of the

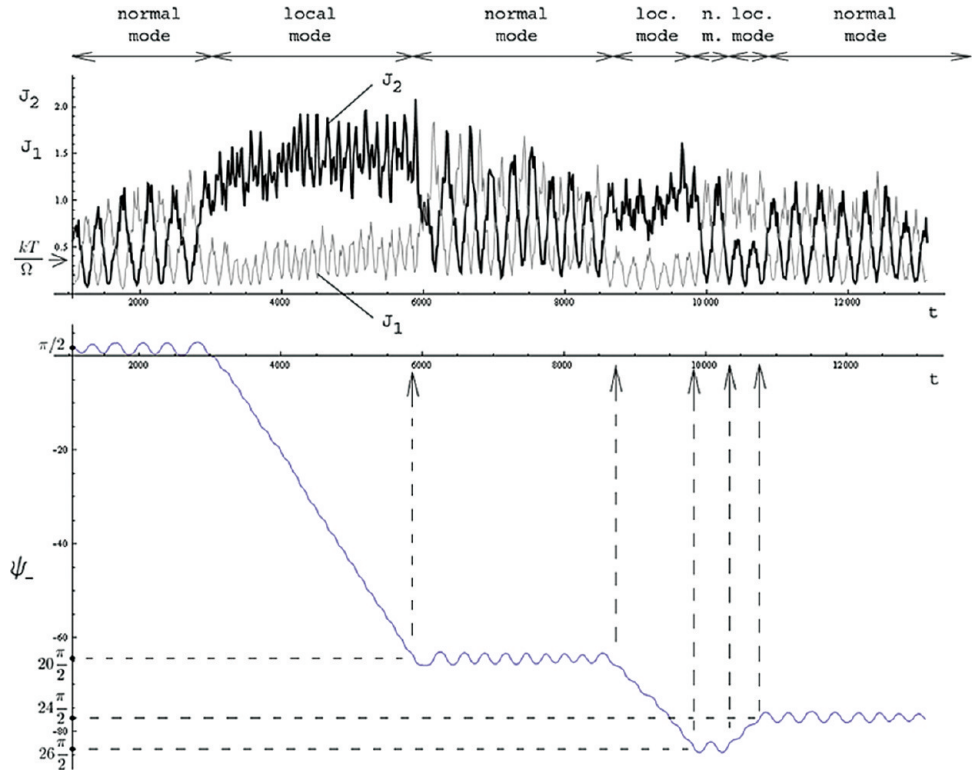

Figure 8. A typical trajectory that shows normal-to-local mode transitions in ABA molecules. The type of local mode here is the L mode. This type of local-mode behavior corresponds to free rotations of the hindered rotor above the cosine potential (see discussion in section II), which can be observed in the bottom plot for $\psi_-(t)$. The value of the action variable that corresponds to thermal energy is indicated in the top plot with an arrow.

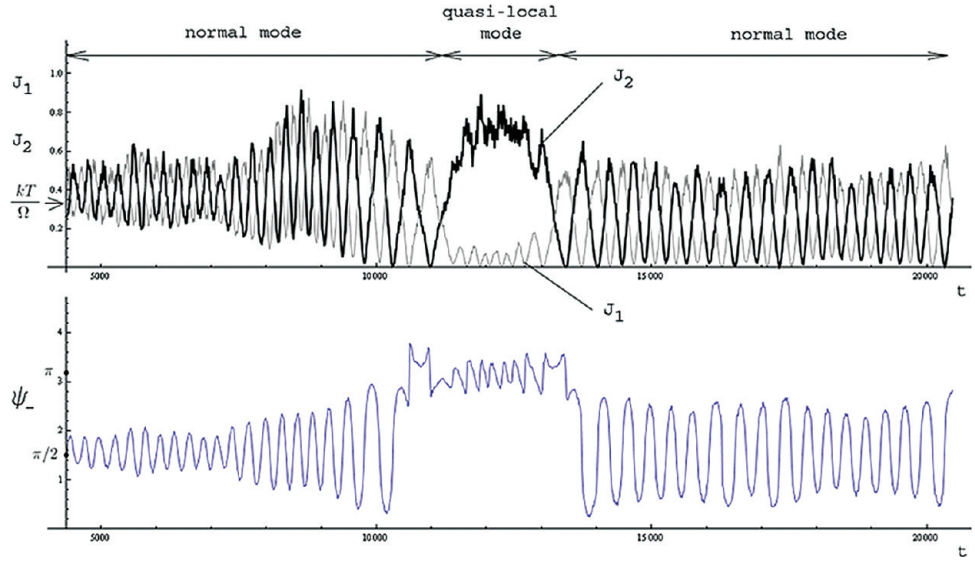

Figure 9. A typical trajectory that shows normal-to-local mode transitions in ABA molecules. The type of local mode here is the QL mode (see section II). In this case, bond vibrational energies become localized; yet, the oscillations of AB and BA bonds are cooperative as ψ_- oscillates around π (in this figure), implying equal phases of AB and BA bond oscillations. The value of the action variable that corresponds to thermal energy is indicated in the top plot with an arrow; the localized vibrational energy is twice the thermal energy.

previous section. The initial value of the total energy and the initial value of J_+ were always placed at thermal equilibrium, that is, $J_+(0) = 2kT/\Omega$. The initial values of J_- and ψ_-, although not so important, were chosen to correspond to the purely antisymmetric normal mode, $\psi_- \equiv (\psi_1 - \psi_2)/2 = \pi/2$, with $J_- = 0$. The initial conditions for the original phase space coordinates $x_1(0)$, $x_2(0)$, $p_1(0)$, and $p_2(0)$ were obtained using the transformations $x_i = x_i(\psi_i, J_i)$ and $p_i = p_i(\psi_i, J_i)$ for the Morse potential.[29] The typical behavior of parameters $\psi_-(t)$, $J_-(t)$, and $J_+(t)$ along the stochastic trajectory of the antisymmetric normal mode of the H_2O model is shown in Figure 11; the periodic oscillations of $J_-(t)$ represent normal-mode energy exchange between AB and BA bonds, and the stable oscillations of $\psi_-(t)$ around $\pi/2$ indicate the antisymmetric normal mode. Figures 8−10 were obtained in a similar way.

In these figures, the dynamic transition events were recorded along a single stochastic trajectory for fixed values of T and γ. The normal-to-local mode transitions were observed using two different methods. The first method is a straightforward "visual" observation, based on recording the moments of time when the

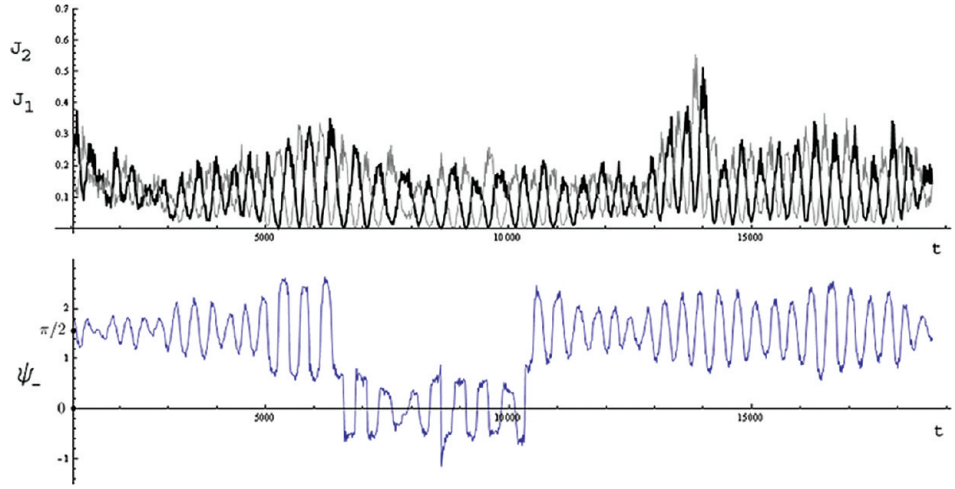

Figure 10. A typical trajectory that shows antisymmetric-to-symmetric normal-mode transitions in ABA molecules. The top plot represents the time dependence of the local action variables J_1 and J_2, while the bottom plot shows the corresponding time dependence of the angle variable ψ_-. The value of ψ_-, that is, half of the difference between the phases of oscillations of AB and BA bonds, changes from oscillations around $\psi_- = \pi/2$ to oscillations around $\psi_- = 0$, indicating the transition from antisymmetric normal-mode to symmetric normal-mode vibrations of the ABA molecule.

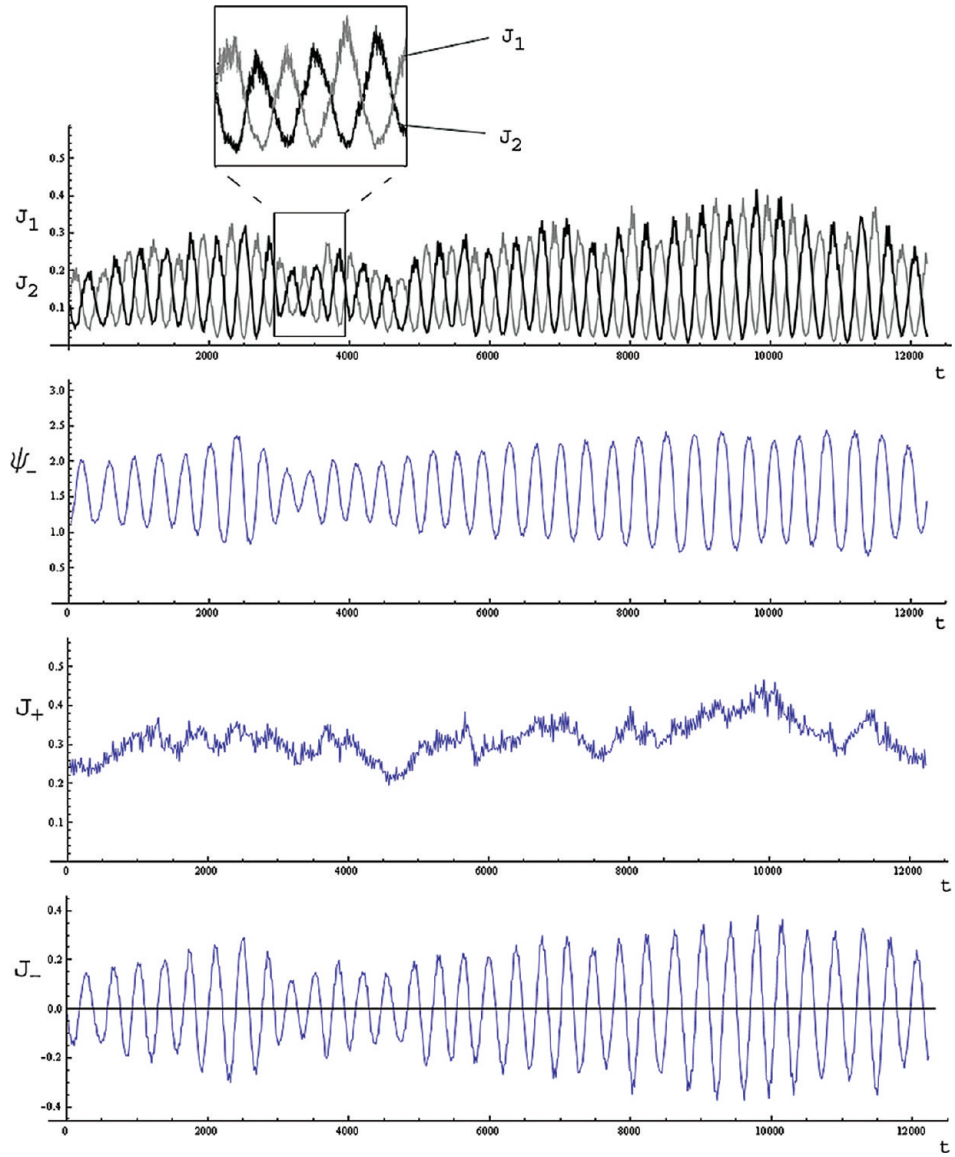

Figure 11. A typical trajectory for the antisymmetric normal-mode oscillation of ABA molecules. The time dependence of the AB bond action J_1 and the BA bond action J_2 is shown in the top plot; as can be seen from the plot, bonds continuously exchange their energies. The middle plot represents the difference between the bond's angle variables; stable oscillations around $\psi_- = \pi/2$ indicate antisymmetric normal-mode behavior. The bottom plot represents equilibrium fluctuations of J_+ along the trajectory.

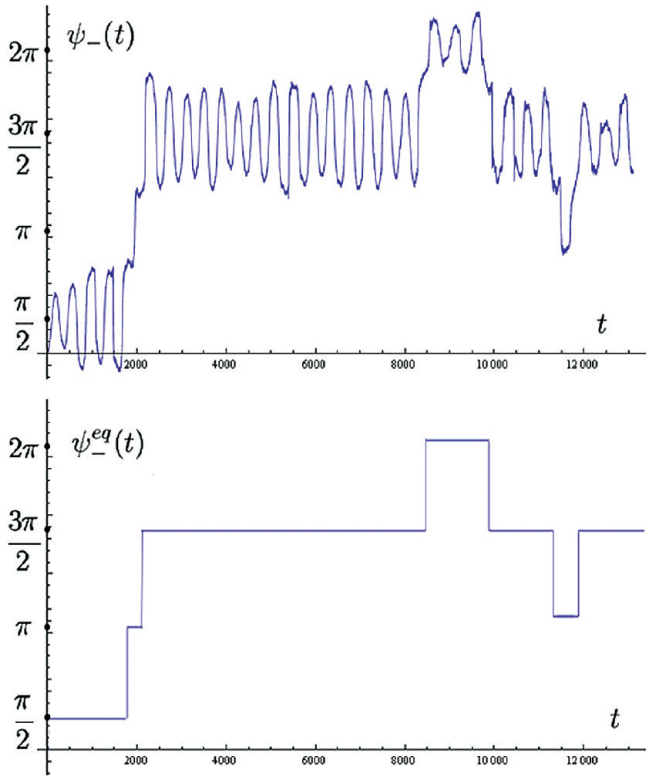

Figure 12. $\psi_-(t)$ and its equilibrium values $\psi_-^{eq}(t)$ for symmetric−antisymmetric normal-mode transitions; the unit of time is 1/Ω.

local bond actions $J_1(t)$ and $J_2(t)$ do not intersect for more than 1.5 of their characteristic oscillation period (eq II.22). The moments when they stop to intersect correspond to the normal-to-local mode transitions, and the moments when they start to intersect correspond to local-to-normal-mode transition (see Figures 8 and 9). The other method to observe normal-to-local mode transitions is to trace the rotor's energy $E_-(t)$ (eq II.4) and to record the moments of time when it becomes larger than $W_0J_+(t)$. This method by itself turns out to be noisy and less reliable than the previous one. In the numerical simulations, we used the combination of two methods to trace normal-to-local mode transitions.

The antisymmetric-to-symmetric (A−S) normal-mode transitions (Figure 10) were observed by tracing the angle variable $\psi_-(t)$ and checking whether the vibrational dynamics is still of the normal-mode type (described in the previous paragraph). The value of ψ_- in the normal-mode vibrations oscillates either around $\pi/2 + \pi k$ (antisymmetric mode) or around the values $\pi + \pi k$ (symmetric mode). Therefore, every time $\psi_-(t)$ oscillating around $\pi k/2$ crosses the points $\pi(k \pm 1)/2$, the A−S or S−A normal-mode transition occurs, depending on whether k is even or odd. By keeping track of every k, it is possible to coarse-grain the A−S and S−A transitions, preserving only the equilibrium values of $\psi_-(t)$, as shown in Figure 12. This allows for easy collection of the statistics of the lifetimes of S and A modes by collecting the statistics of time intervals represented by straight lines in Figure 12. The typical distribution densities of the lifetimes of the A and S modes are shown in Figure 13. One can see a nonexponential decay of the distribution densities, which points to a possible underlying diffusion mechanism that governs dynamic transition. The statistics of times for the local-to-normal-mode transitions were collected using the method described in the previous paragraph. Their typical distribution

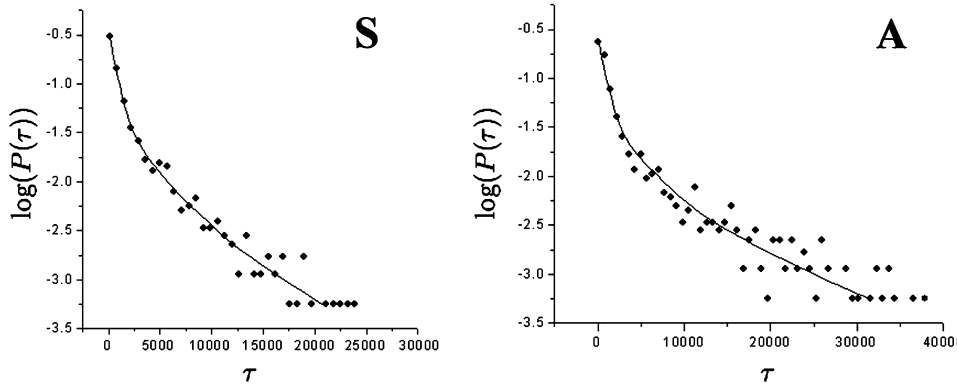

Figure 13. Probability distribution densities for the lifetimes of symmetric (S) and antisymmetric (A) normal modes for the model of H_2O at $kT/D = 1/75$ and $\gamma/\Omega = 1/12000$. Solid lines are the guiding lines for the eye. The unit of time is 1/Ω.

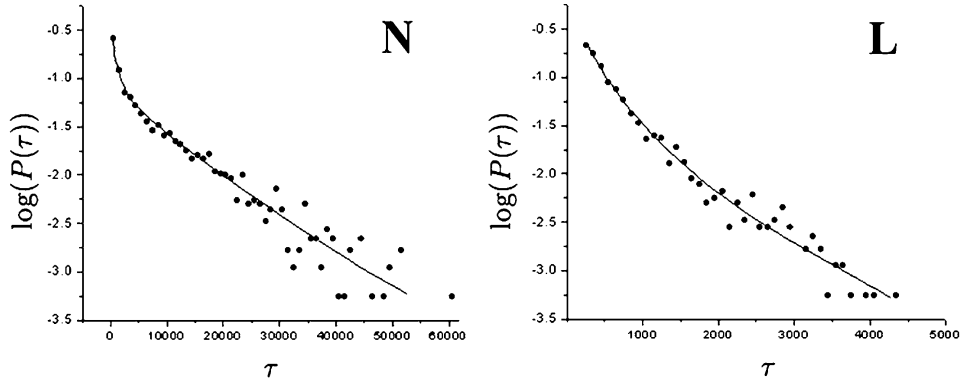

Figure 14. Probability distribution densities for the intervals of time that the H_2O molecule spends in the normal-mode regime (N), that is, in either the antisymmetric or symmetric normal mode, and local-mode regime (L), that is, in either the local or quasi-local mode. The parameters of the simulation were $kT/D = 1/75$ and $\gamma/\Omega = 1/12000$. Solid lines are the guiding lines for the eye.

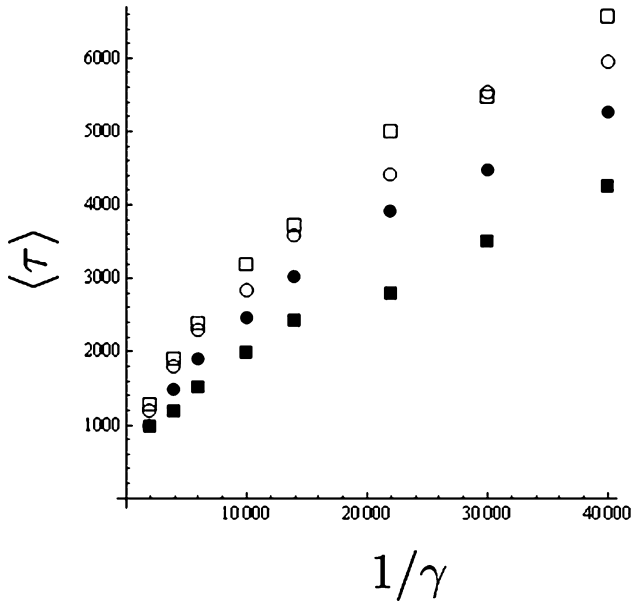

Figure 15. The mean lifetime of the antisymmetric and symmetric normal modes of the model of water molecule as a function of inverse friction in units of $1/\Omega$. Open symbols stand for the antisymmetric normal mode, and solid symbols stand for the symmetric normal mode. Circles represent results for $kT/D = 1/200$, and squares represent results for $kT/D = 1/100$.

densities are shown in Figure 14. Different from the normal-mode distribution density of the lifetimes, the local-mode probability density can be approximately described by a single exponential decay.

We can also calculate the mean lifetime of a particular mode as a function of temperature T and friction coefficient γ. The average times that the H_2O molecule spends in a particular mode along a single trajectory are shown in Figure 15 for different temperatures and friction strengths. The mean lifetime of the antisymmetric and symmetric normal modes monotonically grows with $1/\gamma$, as one should have expected at low frictions. The dependence of the lifetimes on the temperature is weak and is weaker for the antisymmetric normal mode than that for the symmetric normal mode. In the next two papers, we analytically derive the observed numerical results.

V. Discussion

In the present paper, we consider classical vibrational dynamics of an ABA-type molecule represented as the coupled two anharmonic oscillators. The stretching dynamics of the ABA molecule can be effectively reduced to the dynamics of a hindered rotor. Yet, different from the widely used simple pendulum model with a momentum-independent potential, the low-energy regime of the ABA molecule at thermal equilibrium requires explicit consideration of the momentum-dependent rotor potential. The momentum-dependent rotor model not only completely describes the local- and normal-mode behavior of ABA molecules but also captures several interesting phenomena such as the conditional stability of the symmetric normal-mode and the appearance of quasi-local modes. Both local modes and quasi-local modes correspond to the classical localization of vibrational excitations within the AB and BA bonds of the ABA molecule, which remain localized an infinitely long time in the absence of external noise. Yet, while phases of AB and BA bond oscillations are unconstrained in the local-mode regime, they are constrained in the quasi-local-mode regime, similar to the phase locking in the normal-mode case (the reason for "quasi"). The appearance of quasi-local modes is the result of momentum dependence of the potential in the hindered rotor model and is not a result of a higher-order coupling resonance, which otherwise would result in a different relation between local phases φ_1 and φ_2.

The coupling to the environment disturbs the ABA molecules to change its vibrational dynamics. The effect of noise can be viewed from the perspective of Kramers escape mechanism.[40] The normal-mode dynamics of an ABA molecule effectively corresponds to the oscillation of the rotor in the cosine potential. Under the influence of noise, the rotor is perturbed to leave its bounding potential and escapes from it. Since the motion of the rotor above the cosine potential corresponds to local-mode dynamics of an ABA molecule, the effect of noise thus results in the transition from the normal-mode behavior to the local-mode behavior. Once in a local mode, local excitations relax back to their equilibrium energies kT, again forming a normal mode. In this way, switching between normal- and local-mode dynamics is observed in our numerical experiments. In a similar and yet less transparent way, the noise from the environment induces symmetric-to-antisymmetric normal-mode transitions, breaking the symmetry of normal-mode oscillations. The statistics of these transitions was found to be nonexponential, which may indicate an underlying diffusion mechanism. Non-exponential statistics of intramolecular dephasing has been previously observed experimentally[58,59] and in quantum simulations of polyatomic molecules.[60]

In the two subsequent papers,[52,53] we analytically describe the observed noise-induced symmetry-breaking and normal-to-local mode transitions and explicitly derive their statistics.

References and Notes

(1) Child, M. S. *Semiclassical Mechanics with Molecular Applications*; Oxford University Press: New York, 1992.
(2) Noid, D. W.; Koszykowski, M. L.; Marcus, R. A. *Annu. Rev. Phys. Chem.* **1981**, *32*, 267.
(3) Gruebele, M.; Wolynes, P. *Acc. Chem. Res.* **2004**, *37*, 261.
(4) Rice, S. *Adv. Chem. Phys.* **1981**, *47*, 117.
(5) Leitner, D. M.; Wolynes, P. G. *J. Phys. Chem. A* **1997**, *101*, 541.
(6) Lehmann, K.; Scoles, G.; Pates, B. *Annu. Rev. Phys. Chem.* **1994**, *45*, 241.
(7) Margulis, C. J.; Coker, D. F.; Lynden-Bell, R. M. *J. Chem. Phys.* **2001**, *114*, 367.
(8) Campbell, D. K.; Flach, S.; Kivshar, Y. S. *Physics Today* **2004**, *57*, 43.
(9) Sibert, E. L.; Hynes, J. T.; Reinhardt, W. P. *J. Chem. Phys.* **1982**, *77*, 3595.
(10) Sibert, E. L.; Reinhardt, W. P.; Hynes, J. T. *J. Chem. Phys.* **1982**, *77*, 3583.
(11) Schmid, G. M.; Coy, S. L.; Field, R. W.; Silbey, R. J. *J. Chem. Phys.* **1994**, *101*, 869.
(12) Hutchinson, J. S.; Sibert, E. L.; Hynes, J. T. *J. Chem. Phys.* **1984**, *81*, 1314.
(13) Arnold, V. I. *Mathematical Methods of Classical Mechanics*; Springer: New York, 1978.
(14) Lichtenberg, A. J.; Lieberman, M. A. *Regular and Stochastic Motion*; Springer: New York, 1983.
(15) von Zeipel, H. *Ark. Mat., Astron. Fys.* **1916**, *11*, 1.
(16) Gustavson, F. G. *Astron. J.* **1966**, *71*, 670.
(17) Deprit, A. *Celest. Mech.* **1969**, *1*, 12.
(18) Chirikov, B. V. *Phys. Rep.* **1979**, *52*, 263.
(19) Ford, J. *Adv. Chem. Phys.* **1973**, *24*, 155.
(20) Oxtoby, D. W.; Rice, S. A. *J. Chem. Phys.* **1976**, *65*, 1676.
(21) Hutchinson, J. S.; Reinhardt, W. P.; Hynes, J. T. *J. Chem. Phys.* **1983**, *79*, 4247.
(22) Chapman, S.; Garrett, B. C.; Miller, W. H. *J. Chem. Phys.* **1976**, *64*, 502.
(23) Jaffe, C.; Reinhardt, W. P. *J. Chem. Phys.* **1982**, *77*, 5191.
(24) Uzer, T.; Noid, D. W.; Marcus, R. A. *J. Chem. Phys.* **1983**, *79*, 4412, and references therein.
(25) Farrelly, D. *J. Chem. Phys.* **1986**, *85*, 2119.
(26) Child, M. S.; Lawton, R. T. *Faraday Discuss. Chem. Soc.* **1981**, *71*, 273.

(27) Kellman, M. E. *J. Chem. Phys.* **1985**, *83*, 3843.
(28) Li, Z.; Xiao, L.; Kellman, M. E. *J. Chem. Phys.* **1990**, *92*, 2251.
(29) Jaffe, C.; Brumer, P. *J. Chem. Phys.* **1980**, *73*, 5646.
(30) Martens, C. C.; Ezra, G. S. *J. Chem. Phys.* **1987**, *87*, 284.
(31) Stefanski, K.; Pollak, E. *J. Chem. Phys.* **1987**, *87*, 1079.
(32) Stuchebrukhov, A. A.; Marcus, R. A. *J. Chem. Phys.* **1993**, *98*, 8443.
(33) McCoy, A. B.; Sibert, E. L. *J. Chem. Phys.* **1989**, *92*, 1893.
(34) Heller, E. J. *J. Phys. Chem.* **1995**, *99*, 2625.
(35) Jacobson, M. P.; O'Brien, J. P.; Silbey, R. J.; Field, R. W. *J. Chem. Phys.* **1999**, *109*, 121.
(36) Flaud, J. M.; Vaittinen, O.; Campargue, A. *J. Mol. Spectrosc.* **1998**, *190*, 262, and references therein.
(37) Sako, T.; Yamanouchi, K. *Chem. Phys. Lett.* **1996**, *264*, 403, and references therein.
(38) Rouben, D. C.; Ezra, G. S. *J. Chem. Phys.* **1995**, *103*, 1375.
(39) Kellman, M. E.; Tyng, V. *Acc. Chem. Res.* **2007**, *40*, 243.
(40) Kramers, H. A. *Physica* **1940**, 7.
(41) Wiesenfeld, K.; Moss, F. *Nature* **1995**, *373*, 33.
(42) Hanggi, P.; Bartussek, R.; Talkner, P.; Luczka, J. *Europhys. Lett.* **1996**, *35*, 315.
(43) Pikovsky, A. *Phys. Lett. A* **1992**, *165*, 33.
(44) Horsthemke, W.; Levefer, R. *Noise Induced Transition*; Springer: Berlin, 1984.
(45) Parson, R. P.; Heller, E. J. *J. Chem. Phys.* **1986**, *85*, 2569.
(46) Martens, C. C.; Reinhardt, W. P. *J. Chem. Phys.* **1990**, *93*, 5621.
(47) Kryvohuz, M.; Marcus, R. A. *J. Chem. Phys.* **2010**, In press.
(48) Pisarchik, A. N.; Jaimes-Reategui, R. *Phys. Lett. A* **2005**, *338*, 141.
(49) Fugmann, S.; Hennig, D.; Schimansky-Geier, L.; Hanggi, P. *Phys. Rev. E* **2008**, *77*, 061135.
(50) Kawamura, Y.; Nakao, H.; Kuramoto, Y. *Phys. Rev. E* **2007**, *75*, 036209.
(51) Chik, D.; Coster, A. *Phys. Rev. E* **2006**, *74*, 041128.
(52) Kryvohuz, M.; Cao, J. *Chem. Phys.* **2010**, doi: 10.1016/j.chemphys.2010.02.024.
(53) Kryvohuz, M.; Cao, J. **2010**, in preparation.
(54) Silva, L. O. E.; Mendonca, J. T. *Phys. Rev. A* **1992**, *46*, 6700.
(55) Hanggi, P.; Talkner, P.; Borkovec, M. *Rev. Mod. Phys.* **1990**, *62*, 251.
(56) Zwanzig, R. *Nonequilibrium Statistical Mechanics*; Oxford University Press: New York, 2001.
(57) Gardiner, C. W. *Handbook of Stochastic Methods for Physics, Chemistry and the Natural Sciences*; Springer-Verlag: Berlin, Heidelberg, Germany, 2004.
(58) Felker, P. M.; Zewail, A. H. *J. Chem. Phys.* **1985**, *82*, 2975.
(59) Smith, P. G.; McDonald, J. D. *J. Chem. Phys.* **1990**, *92*, 1004.
(60) Gruebele, M. *Proc. Natl. Acad. Sci. U.S.A.* **1998**, *95*, 5965.

JP102675Y